

8. SYNCHROTRON CRYSTALLOGRAPHY

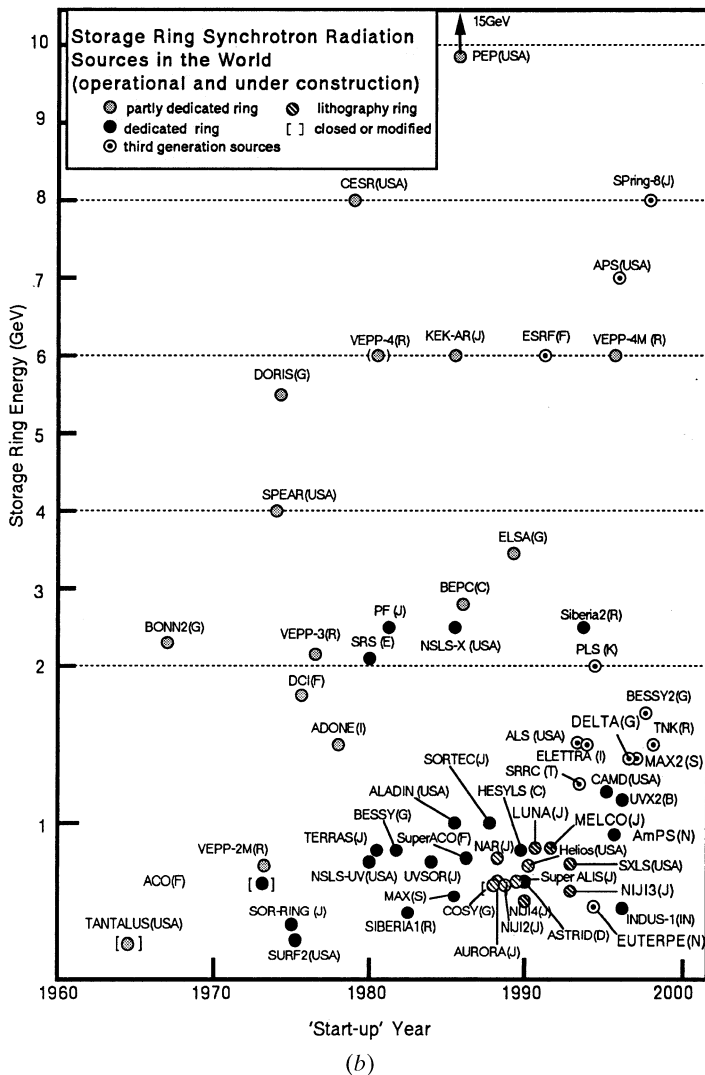
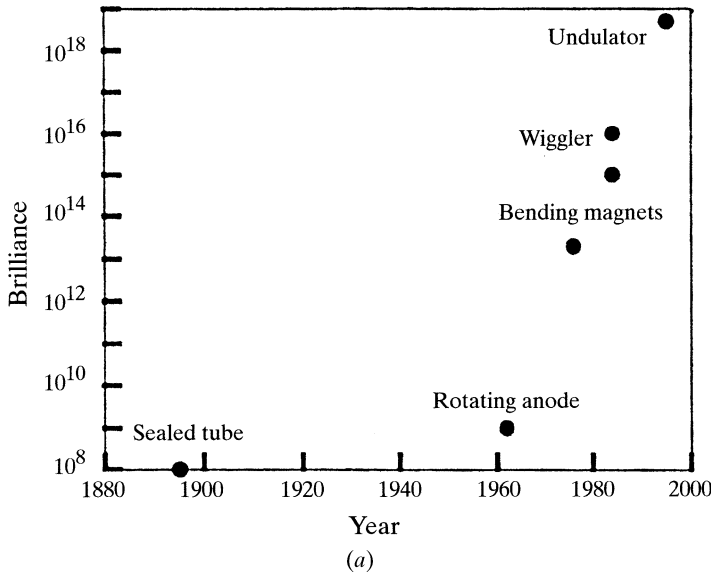


Fig. 8.1.2.1. (a) Evolution of X-ray source brilliance (photons s⁻¹ mrad⁻² mm⁻² per 0.1% Δλ/λ) in the hundred years since Rontgen’s discovery of X-rays in 1895. Adapted from Coppens (1992). (b) The evolution of storage-ring synchrotron-radiation sources over the decades, as illustrated by their increasing number and range of machine energies up to the present (Suller, 1998).

- (2) to increase the available intensity (multipole wiggler);
- (3) to increase the brilliance *via* interference and also yield a quasi-monochromatic beam (undulator) (Fig. 8.1.2.4b shows the distinctly different emission from an undulator);
- (4) to provide a different polarization (*e.g.* to rotate the plane of polarization, to produce circularly polarized light *etc.*).

The classification of a periodic magnet ID as a wiggler or undulator is based on whether the angular deflection, δ, of the electron beam is small enough to allow radiation emitted from one pole to interfere directly with that from the next pole. In a wiggler, δ ≫ γ⁻¹, so the interference is negligible and the spectral emission (Fig. 8.1.2.4a) is very similar in shape to, but scaled up from, the universal curve (*i.e.* bending magnet spectral shape). In an undulator δ ≤ γ⁻¹ and the interference effects are highly significant (Fig. 8.1.2.4b). If the period of the ID is λ_u (cm), then the wavelengths λ_i (*i* integer) emitted are given by

$$\lambda_i = \frac{\lambda_u}{i2\gamma^2} \left(1 + \frac{K^2}{2} + \gamma^2\theta^2 \right), \quad (8.1.3.1)$$

where K = γδ.

The spectral width of each peak is

$$\Delta_i \simeq 1/iN, \quad (8.1.3.2)$$

where N is the number of poles.

The angular deflection, δ, is changed by opening or closing the gap between the pole pieces. Opening the gap weakens the field and shifts the emitted lines to shorter wavelengths, but decreases the flux. Conversely, to achieve a high flux means closing the gap, and in order to avoid the fundamental emission line moving to long wavelength, the machine energy has to be high. Short-wavelength undulator emission is the province of the third-generation machines, such as the ESRF in Grenoble, France (6 GeV), the APS at Argonne National Laboratory, Chicago, USA (7 GeV), and SPring-8 at Harima Science Garden City, Japan (8 GeV). Another important consideration is to cover the entire spectral range of interest to the user *via* the tuning range of the fundamental line and harmonics. This is easier the higher the machine energy. However, important developments involving so-called narrow-gap undulators (*e.g.* from 20 mm down to ~7 mm) erode the advantage of higher machine energies ≥6 GeV for the production of X-rays within the photon energy range of primary interest to macromolecular crystallographers, namely ~30 keV down to ~6 keV.

8.1.4. Beam characteristics delivered at the crystal sample

The sample acceptance, α [equation (8.1.4.1)], is a quantity to which the synchrotron machine emittance [equation (8.1.2.2)] should be matched, *i.e.*,

$$\alpha = x\eta, \quad (8.1.4.1)$$

where x is the sample size and η the mosaic spread. For example, if x = 0.1 mm and η = 1 mrad (0.057°), then α = 10⁻⁷ m rad or 100 nm rad.

At the sample position, the intensity of the beam, usually focused, is a useful parameter:

$$\text{Intensity} = \text{photons per s per focal spot area.} \quad (8.1.4.2)$$

Moreover, the horizontal and vertical convergence angles are ideally kept smaller than the mosaic spread, *e.g.* ~1 mrad, so as to measure reflection intensities with optimal peak-to-background ratio.

To produce a focal spot area that is approximately the size of a typical crystal (~0.3 mm) and with a convergence angle ~1 mrad

8.1. SYNCHROTRON RADIATION

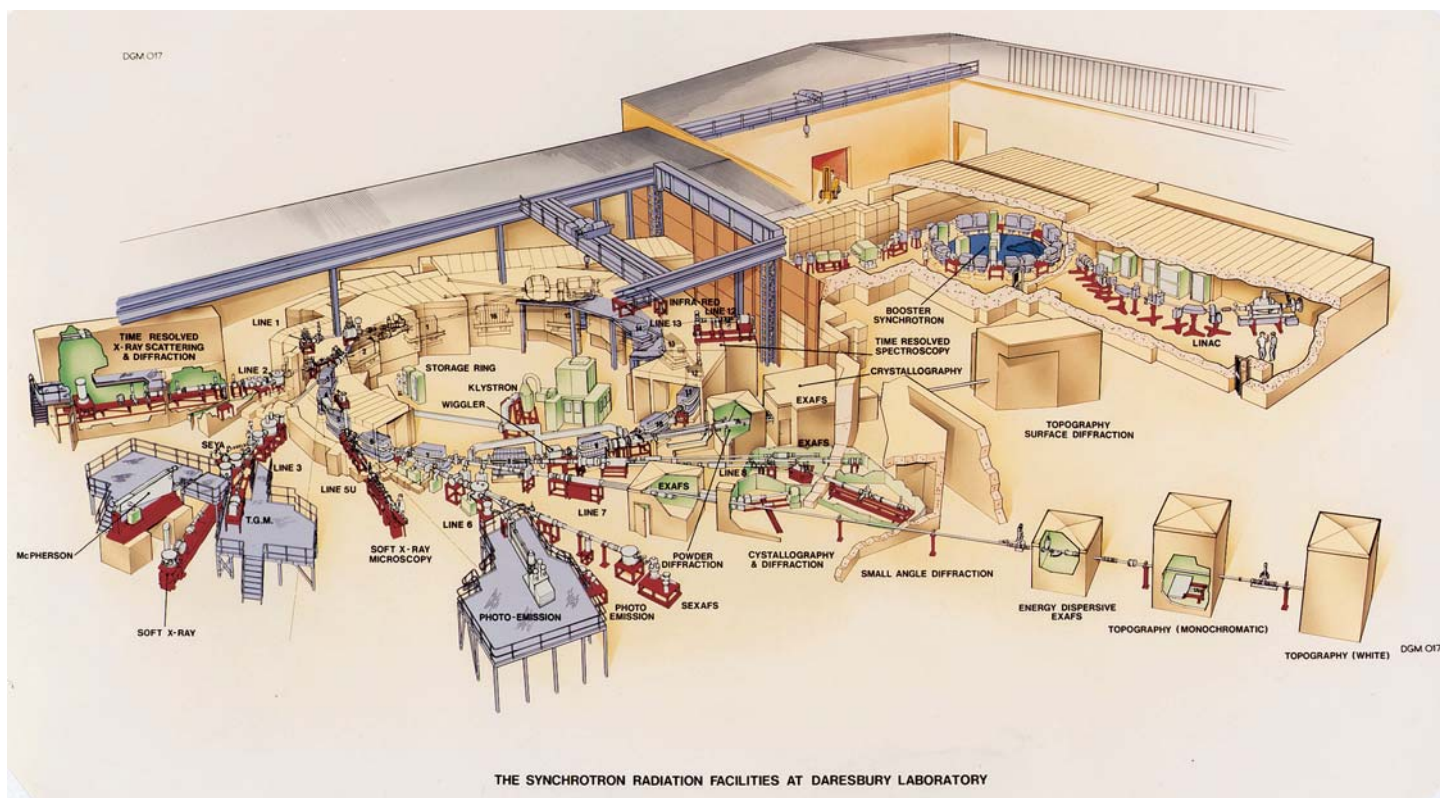


Fig. 8.1.2.2. Overall layout of the Daresbury SRS facility, including LINAC, booster synchrotron, main storage ring and experimental beamlines (as in 1985 for clarity). Reproduced with the permission of CLRC Daresbury Laboratory.

Table 8.1.4.1. Internet addresses of SR facilities with macromolecular crystallography beamlines

Synchrotron-radiation source	Location	Address
ALS, Advanced Light Source	Lawrence Berkeley Lab., Berkeley, California, USA	http://www-als.lbl.gov/als/
APS, Advanced Photon Source	Argonne National Lab., Chicago, Illinois, USA	http://epics.aps.anl.gov/
BESSY	Berlin, Germany	http://www.bessy.de/
BSRF, Beijing Synchrotron Radiation Facility	Beijing, China	http://www.ihep.ac.cn/ins/IHEP/bsrf/bsrf.html
CAMD, Center for Advanced Microstructures and Devices	Baton Rouge, Louisiana, USA	http://www.camd.lsu.edu/
CHESS, Cornell High Energy Synchrotron Source	Ithaca, New York, USA	http://www.chess.cornell.edu/
Daresbury Laboratory CLRC	Daresbury, England	http://www.dl.ac.uk
Elettra	Trieste, Italy	http://www.elettra.trieste.it
ESRF, European Synchrotron Radiation Facility	Grenoble, France	http://www.esrf.fr
HASYLAB DESY, Deutsches Elektronen-Synchrotron	Hamburg, Germany	http://www.desy.de/
LNLS, National Synchrotron Light Laboratory	Campinas, Brazil	http://www.lnls.br/
LURE	Orsay, France	http://www.lure.u-psud.fr/
MAXLab	Lund, Sweden	http://www.maxlab.lu.se/
NSLS, National Synchrotron Light Source	Brookhaven National Lab., New York, USA	http://www.nsls.bnl.gov/
The Photon Factory, KEK	Tsukuba, Japan	http://www.kek.jp/kek/IMG/PF.html
PLS, Pohang Light Source	Pohang, Korea	http://pal.postech.ac.kr/
SLS, Swiss Light Source	Paul Scherrer Institut, Villigen, Switzerland	http://www1.psi.ch/www-sls-hn/
SPring-8, Super Photon Ring	Riken Go, Japan	http://www.spring8.or.jp/
SRRC, Synchrotron Radiation Research Center	Hsinchu City, Taiwan	http://210.65.15.200/en/index.html
SSRL, Stanford Synchrotron Radiation Laboratory	SLAC, California, USA	http://www-ssrl.slac.stanford.edu/
VEPP-3	Novosibirsk, Russia	http://ssrc.inp.nsk.su/

8. SYNCHROTRON CRYSTALLOGRAPHY

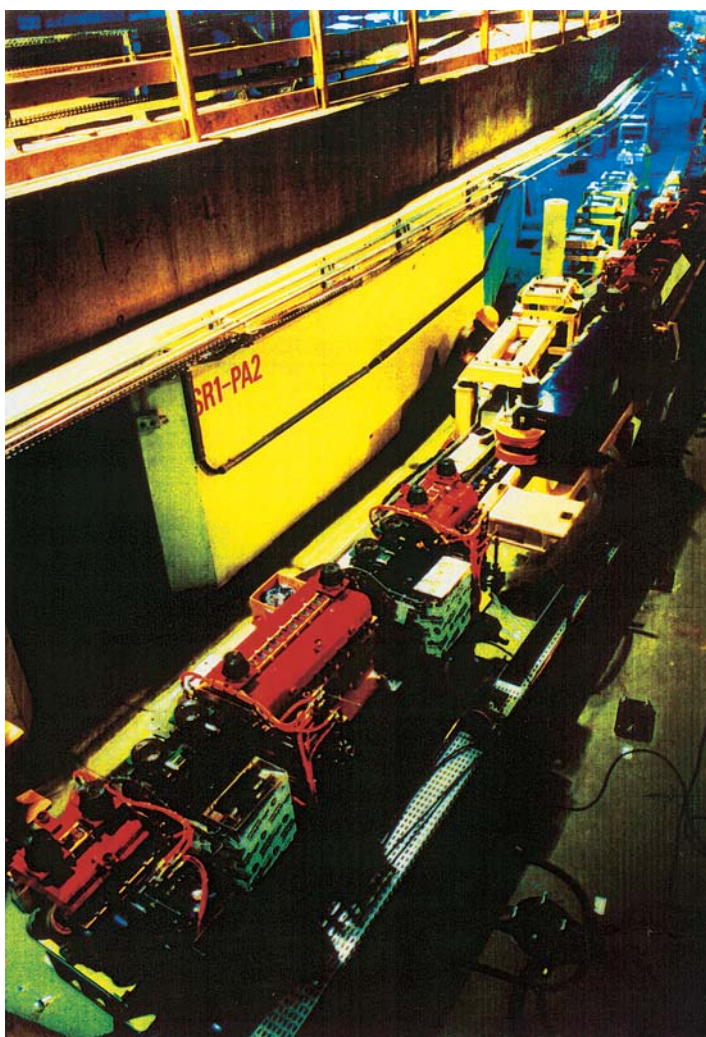


Fig. 8.1.2.3. The ring tunnel and part of the machine lattice at the ESRF, Grenoble, France.

sets a sample acceptance requirement to be met by the X-ray beam and machine emittance. A machine with an emittance that matches the acceptance of the sample greatly assists the simplicity and performance of the beamline optics (mirror and/or monochromator) design. The common beamline optics schemes are shown in Fig. 8.1.4.1.

In addition to the focal spot area and convergence angles, it is necessary to provide the appropriate spectral characteristics. In monochromatic applications, involving the rotating-crystal diffraction geometry, for example, a particular wavelength, λ , and narrow spectral bandwidth, $\delta\lambda/\lambda$, are used. Fig. 8.1.4.2(a) shows an example of a monochromatic oscillation diffraction photograph from a rhinovirus crystal as an example recorded at CHESS, Cornell. Fig. 8.1.4.2(b) shows the prediction of a white-beam broadband Laue diffraction pattern from a protein crystal recorded at the SRS wiggler, Daresbury, colour-coded for multiplicity.

Table 8.1.4.1 lists the internet addresses of the SR facilities worldwide that currently have macromolecular beamlines.

8.1.5. Evolution of SR machines and experiments

8.1.5.1. First-generation SR machines

The so-called first generation of SR machines were those which were parasitic on high-energy physics operations, such as DESY in Hamburg, SPEAR in Stanford, NINA in Daresbury and VEPP in

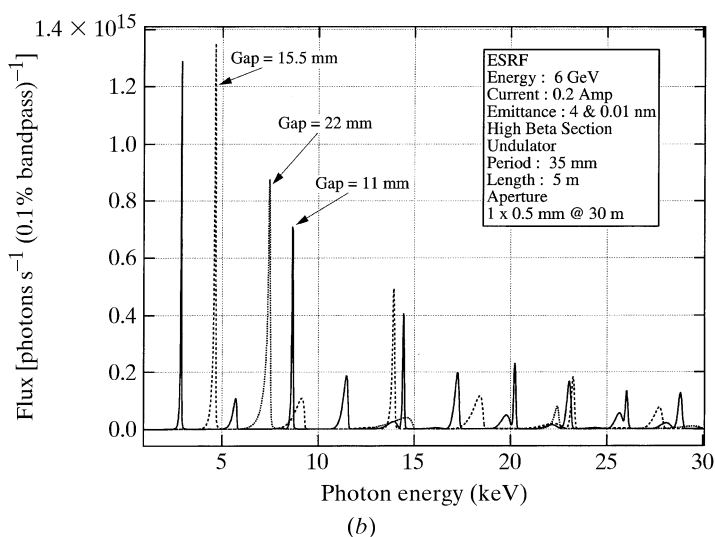
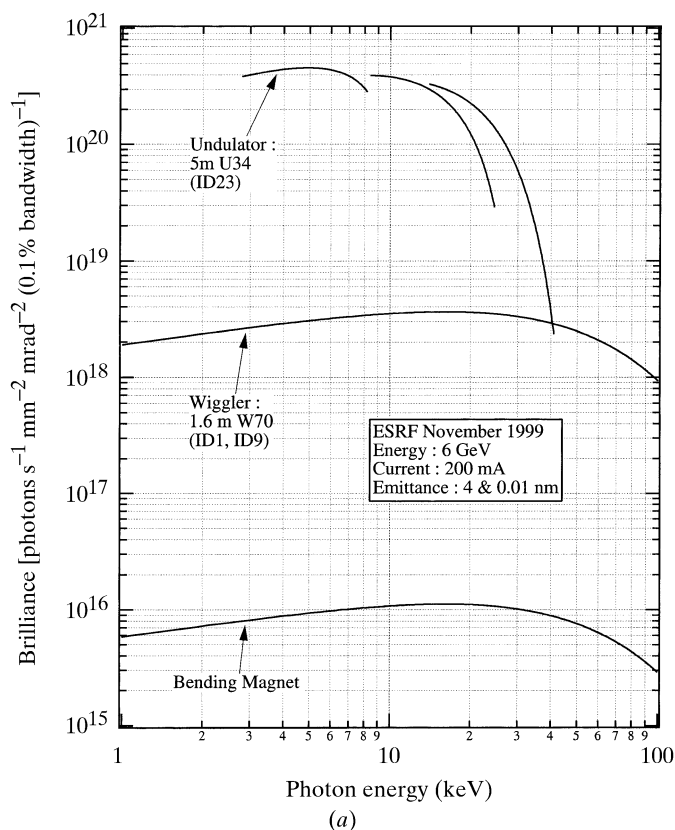


Fig. 8.1.2.4. SR spectra. (a) Brilliances of different SR source types (undulator, multipole wiggler and bending magnet) as exemplified by such sources at the ESRF. For the undulator, the tuning range (*i.e.* as the magnet gap is changed) is indicated. (b) Undulator-emitted spectra at the ESRF, shown as photon fluxes through a 1×0.5 mm aperture at 30 m, for three different gaps, *i.e.* widening the gap shifts the emitted fundamental and associated harmonics in each case to higher photon energies. Kindly provided by Dr Pascal Elleaume, ESRF, Grenoble, France.

Novosibirsk. These machines had high fluxes into the X-ray range and enabled pioneering experiments. Parratt (1959) discussed the use of the CESR (Cornell Electron Storage Ring) for X-ray diffraction and spectroscopy in a very perceptive paper. Cauchois *et al.* (1963) conducted *L*-edge absorption spectroscopy at Frascati and were the first to diffract SR with a crystal (quartz). The opening experimental work in the area of biological diffraction was by Rosenbaum *et al.* (1971). In protein crystallography, multiple-